

## *Chapter 8*

# ADDITIONAL TOOLS FOR SAMPLE-TO-ANSWER POINT-OF-CARE NUCLEIC ACID AMPLIFICATION TESTING

### **Introduction**

The development of a fully-integrated sample-to-answer point-of-care NAAT which meets all of the ASSURED criteria remains a critical challenge for the diagnostics field. NAAT is inherently complex, and to realize a fully-integrated sample-to-answer point-of-care diagnostic requires many components which can perform multiple steps: sample transfer, nucleic acid extraction, nucleic acid amplification, readout, and analysis. Each component must fulfill the ASSURED criteria individually (e.g. Affordable, User-friendly, Rapid, Robust, Equipment-free, Deliverable). These characteristics must further be retained when these components are combined, and the fully-integrated test must additionally be Sensitive and Specific. A system which integrates all of these components while meeting performance requirements has yet to be realized.

In this chapter, I develop a fully-integrated sample-to-answer point-of-care NAAT kit.<sup>1</sup> The test kit is composed of the following components: (1) meter-mix device presented in Chapter 4, (2) sample preparation module, (3) amplification module, (4) cell-phone readout, (5) automated MATLAB image processing, and (6) an automated base station. I will elaborate on the design of each component (with the exception of the meter-mix device) followed by an evaluation of integrated device performance.

### **Sample preparation module**

EJ designed the simultaneous pre-pressurization pumping lid approach and contributed to sealing surface improvements. Created the 6x pressure sensor capable of measuring all chambers simultaneously using an adaptation of David Selck's previously developed LabView script.

Daan Witters, Stefano Begolo, and Feng Shen all contributed to the design of the sample preparation module.

### *Design*

The sample preparation module takes lysed sample (mixed with Zymo buffers DNA/RNA shield and DNA/RNA lysis buffer) as input. Both DNA and RNA are purified on a silica column using NA extraction buffers and eluted with either water or Tris-EDTA (TE) buffer. There are three innovations which improve the performance of the sample preparation module over existing centrifugation protocols. First, the sample preparation module uses an additional two-phase wash buffer as presented in Chapter 2, which improves extraction purity. Secondly, the sample preparation module uses positive pressure to push liquids through the column rather than a centrifugation. This allows the sample preparation module to be smaller, more portable, and 3D-printed. Lastly, the sample preparation module uses SlipValve technology, which reduces user interactions resulting in a quick 4-min extraction.

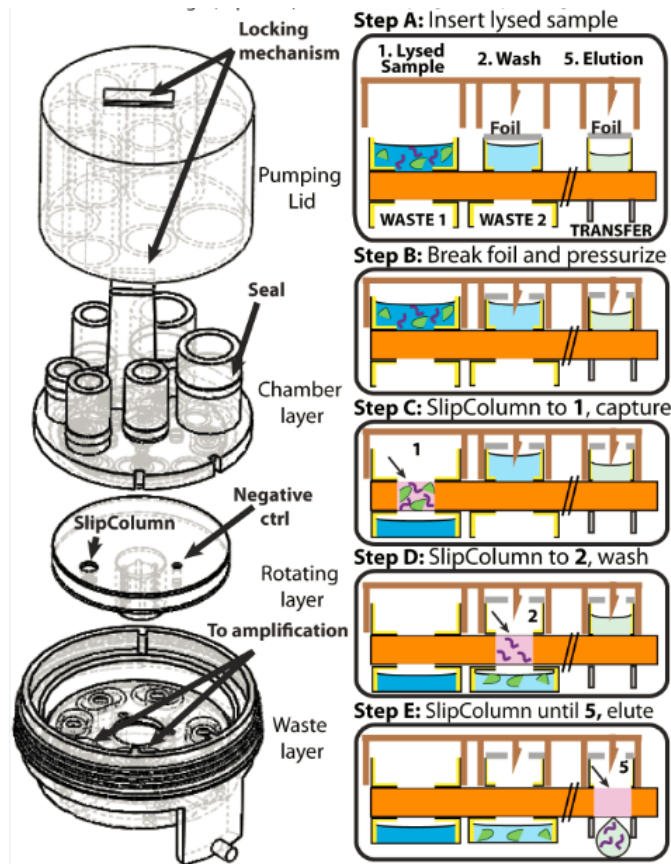


**Figure 1.1: Sample preparation module design**

(left) Solidworks exploded view showing pumping lid to generate and hold positive pressure, chamber layer to hold (1) lysed sample, (2) Zymo viral wash buffer, (3) 1-undecanol two-phase wash, (4) air push, (5) elution, and (6) negative control, rotating layer which houses the SlipColumn, and a waste layer to capture flow-through waste. (right) Schematic showing the steps to use the sample preparation module. The user adds the lysed sample (step A), pushes down the pumping lid (step B), and presses start (steps C-E).

### *Pressurization and SlipValving*

The positive pressurize mechanism works by pushing the pumping lid onto the chamber layer. In this moment, all 6 chambers are simultaneous pre-pressurized and the pumping lid locks into place due to the snap-fit feature. Because the chambers are well-sealed, the

pressure in each chamber is maintained over the course of the 4 min extraction. When the user presses start, the motor of the base station activates the rotating layer, bringing the SlipValve (containing the silica column) below each chamber sequentially. Once the SlipValve transits below the first chamber where the lysed sample is stored, the lysed sample pushes through the silica column thereby binding DNA and RNA to the column. The motor pauses to allow all of the lysed sample to pump through to the waste layer, and then the motor automatically rotates again to the next position to pump through wash buffer. This repeat until the elution step, and the elution containing purified DNA and RNA routes automatically to the amplification module.

### *Holding Pressure Validation*

To ensure that pressure is held in each chamber, I developed a pressure sensor capable of measuring the pressure in all six chambers in real-time. The pressure sensor software was developed in LabView (adaptation of program originally programmed by Dr. David Selck), and the pressure sensors were physically wired on a solderable prototyping board. After placing the pumping lid, we observed that the pressure held constant for at least 30 min. When the base station operates the rotating layer according to the pre-programmed rotation schedule, a pressure drop is observed at the appropriate time (**Figure 1.2**).

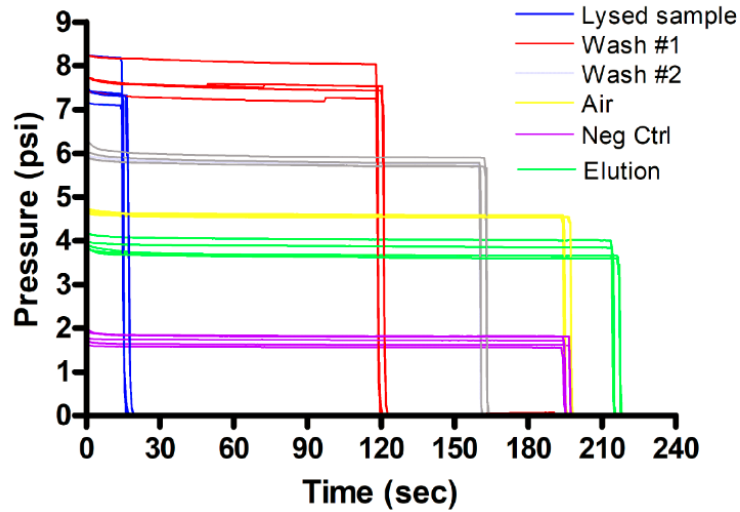


**Figure 1.2: Sample preparation module holding pressure validation**

Four repeated experiments showing the initial pre-pressurization of six chambers by placing the pumping lid onto the sample preparation module. The motor automatically moves the rotating layer and SlipValve below each chamber at the pre-programmed time.

### Parallel-filled amplification module

EJ designed the parallel-filling to dead-end hydrophobic membrane strategy. EJ contributed to material selection and assembly practices

DW (Daan Witters) contributed to material selection and assembly practices

### *Design*

Here we present the design for an easy-to-fabricate 5-plex uL volume SlipChip for running NAAT reactions. There are 2 inlets, one for the test which accesses 3 of the 5 wells and one for the control which accesses the remaining 2 wells. The bottom plate have 5 wells where lyophilized reagents (LAMP) are pre-stored. The top plate has channels from the inlets to

each well and from each well to a separate outlet. The outlet has a hydrophobic membrane to allow air to escape but blocks the flow of fluid. This strategy allows parallel filling whereby a single input fluid fills many wells at once, each containing its own set of lyophilized reactants. After well filling, the device is slipped rotationally to isolate each well. With this design, we expect no cross-contamination of rehydrated amplification reagents between different wells. Features on the outer edge of the device constrain slipping to rotation.

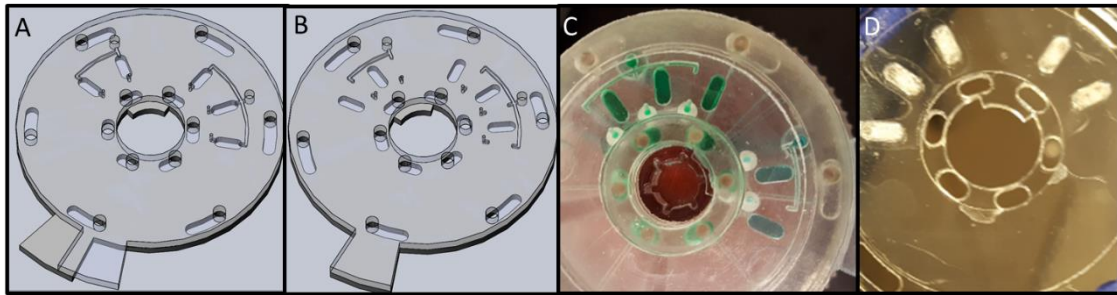


**Figure 1.3: Parallel filling of amplification modules.**

(A-B) Solidworks 3D models of parallel filling amplification modules in (A) unslipped and (B) slipped positions. (C) Parallel filling of the amplification module integrated with multi-chamber sample preparation module and filled with green (representing eluent) and blue (representing negative control) dyes. The multi-chamber pumping lid from the sample preparation module provides the filling pressure. (D) LAMP reagents lyophilized in the wells of the bottom plate.

#### *Fabrication and assembly*

The geometry of the amplification module was designed in CAD software and fabricated using a combination of laser cutting (Epilog Zing 24) and multi-material 3D printing. There are 4 primary components: (i) top plate, (ii) bottom plate, (iii) inner and outer pins, and (iv) inner and outer clamps. A layer of 3M 300 LSE was laminated on the top and bottom side of the bottom plate. The top (2.1 mm) and bottom plates (1.5mm) were laser cut from cast acrylic (McMaster), using vector cutting to generate the outline, wells, and outlets and using

engraving for the channels. A laser-cut donut of 0.175mm PMMA (Goodfellow Cambridge Limited) was attached to the bottom 300LSE on the bottom plate. A thin coat of Krytox GPL 205 was applied by smearing Krytox between two glass slides and stamping the top 300LSE of the bottom plate with Krytox. The appropriate LAMP mix (see below) was added to each respective well and bottom plates were lyophilized overnight. The bottom side of the top plate (without 300LSE) was smeared with a thin layer of Krytox GPL 205. A layer of pre-cut 300LSE that matches the top plate pattern was attached to the top plate. 3 mm discs polypropylene hydrophobic membranes (Sterlitech, 0.22 micro) were applied to the top 300LSE of the top plate to cover the well outlets.

For lyophilization, the 2.5% mannitol was added to the LAMP reaction, glycerol-free Bst 2.0 and AMV RT were used, and the addition of water was minimized. The AdVantage Pro EL lyophilizer shelves were set to precool at -50C with frost seal. Bottom plates were placed onto a tray and inserted into the lyophilizer. The lyophilizer performed thermal treatment by holding -50 °C with 75 min ramp and 60 min hold. Drying had 4 steps: -45 °C with 0 min ramp, 840 min hold at 100 mTorr, -20 °C with 60 min ramp, 5 min hold at 100 mTorr, 0 °C with 60 min ramp, 5 min hold at 100 mTorr, and 25 °C with 120 min ramp, 60 min hold at 100 mTorr. Product was held at 25 C and 100 mTorr until removed from the lyophilizer.

Following lyophilization, bottom plates were removed from the lyophilizer under dry nitrogen and placed into a dry nitrogen glove bag. Bottom and top plates were sandwiched together, and mostly assembled except the final clamping step using the 3D printed inner and outer pin and clamp sets. Nearly assembled amplification modules were stored with desiccant and vacuum sealed (Weston Pro-2300) under dry nitrogen in mylar bags (4 mil).

### *Validation*

To validate the stability of the lyophilized reagents in the amplification module, purified nucleic acids from *Neisseria Gonorrhoeae* at 500 CFU/mL and nuclease-free water were used to rehydrate the lyophilized reagents on the amplification module. Real-time imaging

was used to monitor the RT LAMP reaction in the amplification module. As shown in **Figure 1.4**, the wells containing purified nucleic acids (“positive wells”) displayed increased fluorescence, with a TTP of 13.6 min, compared with 11.6 min when using standard liquid LAMP reagents in an ECO plate. The observed 2 min delay is presumably due to the delay in heating of reagents in our amplification module (~90 sec) compared with the standard ECO-machine (Illumina) heating elements.

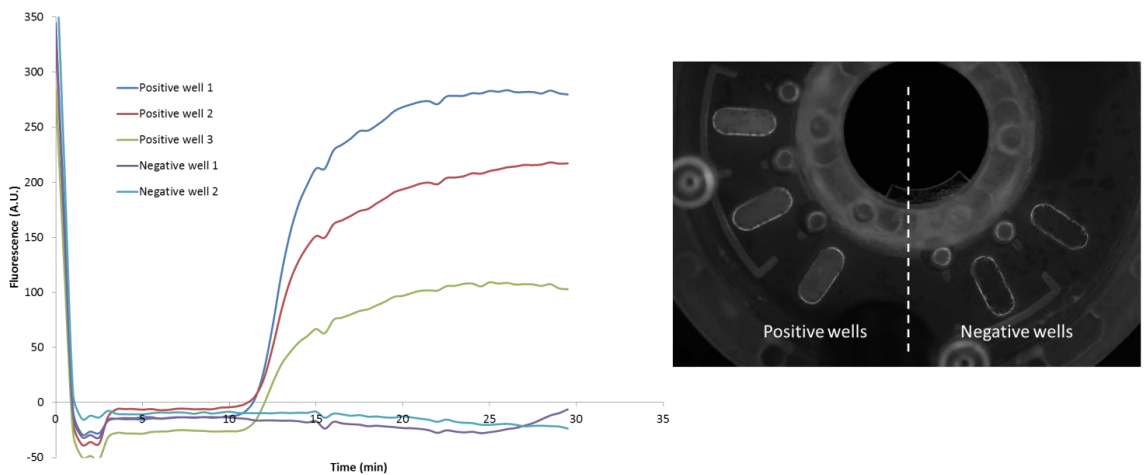


**Figure 1.4: (A) Amplification data and (B) fluorescence image showing real-time imaging of an amplification module that contained lyophilized reagents for the detection of NG.**

The positive wells of the amplification module were loaded with purified nucleic acids from NG, whereas the negative wells were loaded with nuclease-free water. The time-to-positive for the positive wells was 13.6 min, whereas there was no significant increase in fluorescence intensity in the negative wells.

### Cell-phone readout and automated analysis

EJ designed and printed the cell-phone dongle and programmed the MATLAB code.

A cell-phone dongle was designed, 3D printed, and painted black to block out ambient light. The sample preparation and amplification module assembly directly connects to the cell-phone dongle to allow fluorescent readout of the wells. The cell-phone dongle is powered by connecting to the base station. A blue LED passes through a blue filter and shines onto each well. A cell-phone with a yellow filter on the camera is placed onto the dongle and a photo was taken. Following image capture, the photo is automatically uploaded to the cloud for automated image analysis and email delivery of results.

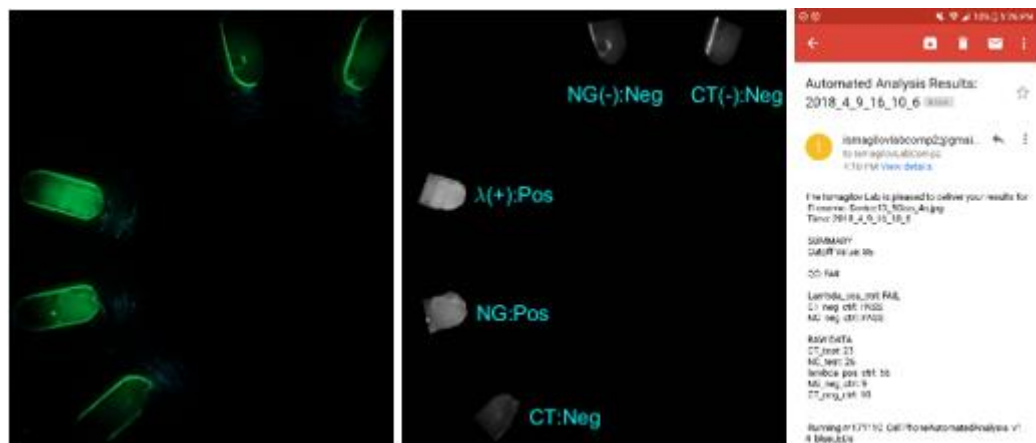


**Figure 1.5: Automated cell-phone image processing.**

(Left) un-processed cell-phone image, (middle) MATLAB processed image, and (right) automated email delivery of results.

### **Automated base station**

AS (Andrey Shur) designed the basic circuit and Arduino code for rotation and heating

EJ further modified the circuit, Arduino code, integrated the base station with other components, and validated the device.

We have successfully built a prototype base station controlled with an \$8.50 Arduino Mini Pro operating on 6 AA rechargeable battery pack which performs combined heating and rotations (**Figure 1.6A**). Power may alternatively be provided by an AC adapter which has greater voltage and amperage capabilities. Heating is performed with a proportional control algorithm, thermistor, and thin-film heater attached to an aluminum disk for even heat distribution. The heater reaches 68°C within 95s and is capable of maintaining temperature within a range of 1°C for at least 40 min. Rotation is controlled by the Arduino and a \$5 Polulu DRV8880 Motor Driver connected to a bipolar-modified 28BYJ-48 stepper motor with a 3D-printed gear train (gear ratio of 11.3). Using a TRH605 Futek Torque Sensor, we measured base station output torque at 1.1 N-m and the torque required to turn the SlipColumn at 0.7 N-m. The base station rotation is responsible for controlling the position of the slip valve of the sample preparation module and for automated slipping of the amplification module (by rotating in the opposite direction). The motor draws little power, and its full sequence (6 rotations and slipping) can be run at least 40 times without recharging. The base station could instead be designed to operate using an AC power supply, which has fewer power restrictions.

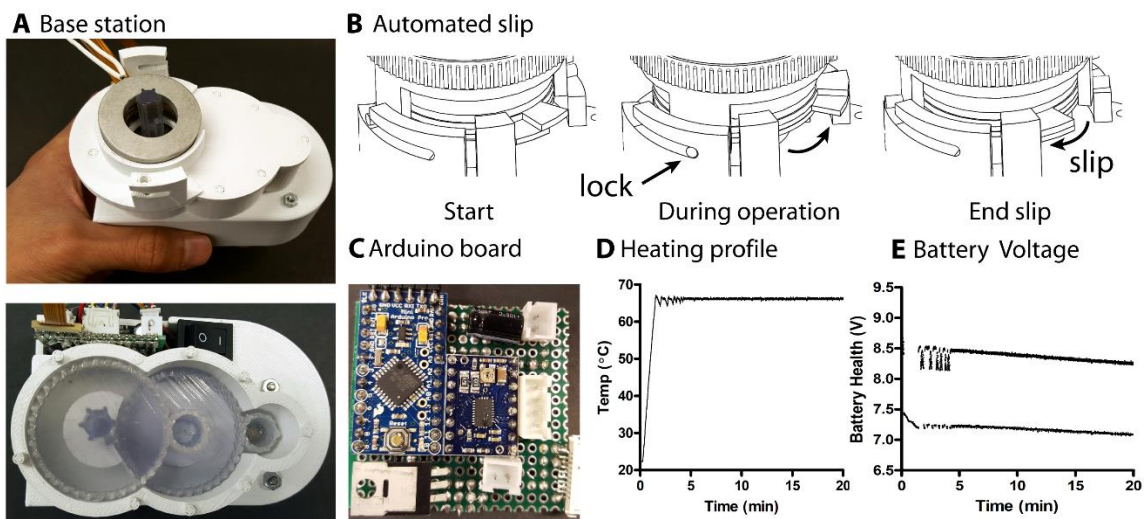


**Figure 1.6: Automated base station components.**

(A) Angled-view and top-down view of the gear rotation mechanism. (B) 3 panels showing automated slip step using rotation. (C) A photo of the Arduino board. (D)

Heating profile measured by Arduino and a thermistor connected to the heater. (E) A measure of battery voltage over time. Under no-load, the voltage is high (8.5 V) and while heating the voltage drops (7.5). Voltage switching is rapid giving the appearance of two curves.

### Integrated device performance

We tested three sample-to-answer experiments using the NAAT kit and either *Chlamydia Trachomatis* (CT), *Neisseria Gonorrhoeae* (NG), or both pathogens spiked into normal human donated urine samples at 5000 CFU or IFU/mL. We found that the kit accurately detected the CT samples, but sometimes the kit failed to detect the NG samples (**Figure 1.7**). Follow-up experiments also confirmed this result. After analyzing the number of NA copies we would expect to find in the final LAMP reaction (stock concentration times input volume times extraction efficiency times reaction volume divided by elution volume), we calculated that there would be up to 340,000 NG RNA copies. For a lyophilized LAMP reaction, we measured a limit-of-detection around 4000 copies. Therefore, our assay kit sometimes failed to detect NG even though we expect 85x more copies than the limit-of-detection.

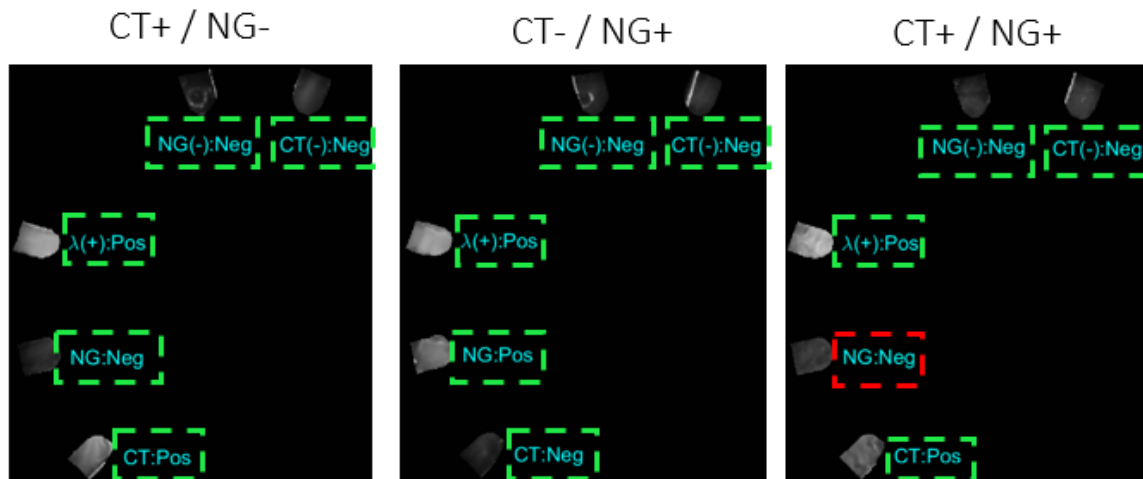


**Figure 1.7: Integrated NAAT kit performance**

(left) Accurate detection of CT at 5000 IFU/mL in a urine sample on the integrated NAAT kit platform. (middle) Accurate detection of NG at 5000 CFU/mL. (right)

Accurate detection of CT at 5000 IFU/mL but inaccurate detection of NG at 5000 CFU/mL.

## **Conclusions**

In this chapter, we demonstrated a fully-integrated sample-to-answer device capable of processing 250  $\mu$ L of urine sample. The NAAT kit is portable with a total weight of less than 1 kilogram and can be held in the palm of a hand. The NAAT kit is rapid with a total assay time of 26 min. Lastly, the NAAT is easy-to-use with 1 min of hands-on time at the start of the assay and 30s hands-on time at the end. With this NAAT kit, we have nearly met our requirements for fulfilling the desired ASSURED criteria.

However, we observed that our assay sensitivity was lacking. In some (but not all) cases, we were unable to detect *Neisseria Gonorrhoeae* at a concentration that we expected to be 85x higher than our limit-of-detection. We suspect this is due to the greater carry-over of extraction buffers when using a pressure-based approach as compared to centrifugation. In Chapter 2, I demonstrated how extraction buffer carry-over can be mitigated by the addition of the two-phase wash. The next step of this project is to more carefully examine extraction buffer carry-over using the sample preparation module by applying similar experimental techniques from Chapter 2 (carefully controlled experiments which will determine the extent of carry-over). I anticipate that once buffer carry-over is characterized and understood, it will be possible to further reduce buffer carry-over by adjusting pressures, modifying the two-phase wash conditions, and/or changing device geometry. I am hopeful that these changes could improve the sensitivity of the NAAT kit, thereby meeting all of the ASSURED criteria for a sample-to-answer POC molecular test.

## **References**

1. D. Witters, E. Jue, N.G. Schoepp, S. Begolo, J. Rodriguez-Manzano, F. Shen, H. Maamar, A. Shur, and R.F. Ismagilov “Autonomous and portable device for rapid

sample-to-answer molecular diagnostics at the point-of-care". Poster presentation at MicroTAS 2017, Savannah, Georgia, Oct. 2017